Reaction Mechanism of Linuron Degradation in TiO_2 Suspension under Visible Light Irradiation with the Assistance of H_2O_2

Y. F. RAO AND W. CHU*

Department of Civil and Structural Engineering, Research Centre for Urban Environmental Technology and Management, The Hong Kong Polytechnic University, Hung Hom, Kowloon, Hong Kong

Received May 6, 2009. Revised manuscript received June 17, 2009. Accepted July 2, 2009.

The application of TiO_2/H_2O_2/Vis (visible light) process for the aqueous degradation of linuron (LNR) has been investigated. The performance of TiO_2/H_2O_2/Vis process has been compared with other processes such as TiO_2/H_2O_2 in the dark, TiO_2/Vis, and H_2O_2/Vis in terms of LNR decay. The result showed that more than 70% LNR could be decomposed in the TiO_2/H_2O_2/Vis. The degradation mechanism of LNR by TiO_2/H_2O_2/Vis process has been verified through investigation of the effects of various radical scavengers on the performance of this system, monitoring the generation of photocurrent, and comparing the intermediates and decay pathways of LNR by UV-TiO_2 and TiO_2/H_2O_2/Vis processes with 16 and 17 intermediates identified, respectively. It has been revealed that demethoxylation and demethylation through alkylic-oxidation is the major mechanism of LNR degradation while dechlorination (hydroxylation at the chlorine site) and direct hydroxylation on the benzene ring is minor in both processes. Mineralization and release of chlorine and nitrogen have been also studied.

Introduction

TiO_2-induced photocatalysis has attracted intensive attention as a water and wastewater treatment technology to eliminate toxic and recalcitrant organic compounds over the past decades due to its particularly optical properties, innocuity, low cost, and enduring stability in terms of photo and chemical corrosion (*1, 2*). The widespread use of TiO_2 as an effective photocatalyst in practical application, however, has been curbed by its optical property that TiO_2 is only sensitive to UV light (*3*). The sun can furnish an abundance of photons; however, UV light only accounts for a small portion (∼5%) of the sun spectrum in comparison to the visible region (∼45%). Therefore, efforts have been devoted to shift the optical response of TiO_2 from the UV to the visible spectral range to effectively utilize solar energy. In recent years, doping (transmit metal and nonmetal) and dye-sensitization technologies have demonstrated successful performance in either narrowing the band gap of TiO_2 or sensitizing photocatalytic properties of TiO_2 toward visible light irradiation (*4*−*8*). It has also been reported that the oxidation reaction of organic compounds occurs even under irradiation of visible light when TiO_2 particles are used as photocatalyst with the addition of H_2O_2 (*9*−*11*). It is known that the chemisorption of H_2O_2 on the surface of TiO_2 can result in the formation of yellow complex "Titanium peroxide" (*12*). Ohno et al. proposed that the epoxidation reaction of 1-decene could be initiated by a photochemical reaction of Ti-η^2-peroxide with 1-decene (*9*). On the other hand, the formation of active hydroxyl radicals was proven in TiO_2/H_2O_2 suspension under visible light irradiation in the work of Li et al. (*10*). They proposed a possible mechanism of the generation of hydroxyl radicals in this system. Titanium peroxide complex formed on the TiO_2 surface could extend the photoresponse to the visible region and can be excited by visible light. The excited surface complex injects an electron to the conduction band of TiO_2. The electrons on the conduction band of TiO_2, then, further initiate the decomposition of H_2O_2 to produce hydroxyl radicals. Although the interaction between H_2O_2 and TiO_2 is well-documented, the oxidation mechanism of organic compounds in the TiO_2/H_2O_2 system under visible light irradiation is not well-understood.

Linuron (LNR) was chosen as a probe compound in this study. LNR, one of the most important phenyl-urea herbicides, has received increasing concern in recent years due to its toxicity, frequent detection in surface and ground waters, and possible endocrine disrupting properties of it and/or its metabolites (*13*−*15*). Therefore, various treatment techniques have been developed to remove LNR in the aqueous phase, including biological methods (*14, 16*), direct photolysis (*17*), O_3/H_2O_2 (*18*), photo-Fenton procedure (*13, 19*), UV/H_2O_2 (*20*), and photocatalysis under UV irradiation (*21*). The study on the TiO_2-based photocatalytic decay of LNR in the presence of H_2O_2 under visible light, however, is limited.

In view of these, this study will focus on the photocatalytic decomposition mechanism of LNR under visible range irradiation with the assistance of H_2O_2.

Experimental Section

Materials. Linuron (3-[3, 4-(dichlorophenyl)-1-methoxy-1-methylurea]) (99%) was obtained from SUPELCO. 1-(3,4-dichlorophenyl)-3-methylurea (DCPMU) and 1-(3,4-dichlorophenyl)urea (DCPU) were purchased from SIGMA-Aldrich. The TiO_2 powder used was Degussa P-25, which contains 80% anatase and 20% rutile verified and confirmed by X-ray analysis. The H_2O_2 (35% in solution) and titanium oxide sulfate hydrate ($TiO(SO_4 \cdot X)H_2O$) were purchased from Riedel-

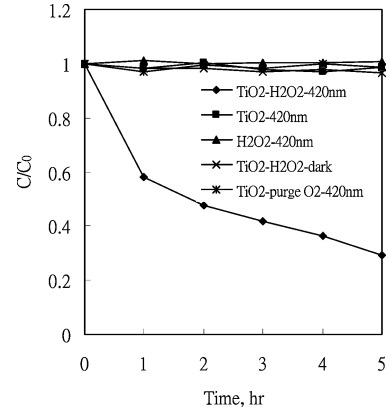

FIGURE 1. LNR degradation under different reaction conditions (Notes: initial LNR concentration is 0.1 mM, TiO_2 loading is 0.6 g/L, the initial concentration of H_2O_2 is 10 mM, initial pH value is 6.0).

* Corresponding author tel: +1-852-2766-6075; fax: +1-852-2334-6389; e-mail: cewchu@polyu.edu.hk.

10.1021/es901333h CCC: $40.75
Published on Web 07/13/2009

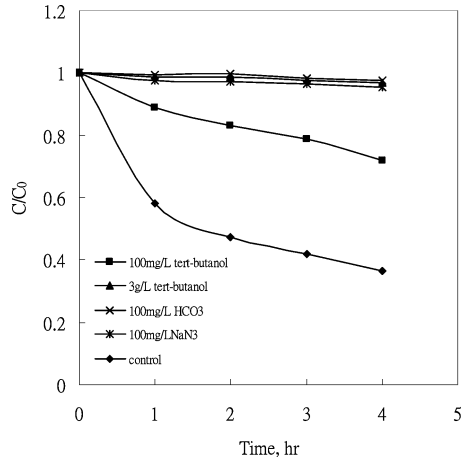

FIGURE 2. Effect of radical scavenger on visible-light photocatalysis of LNR with the assistance of H_2O_2 (initial LNR concentration is 0.1 mM, TiO_2 loading is 0.6 g/L, the initial concentration of H_2O_2 is 10 mM, initial pH value is 6.0).

deHaën and International Laboratory, respectively. All other chemicals were analytic purity and all solvents were HPLC grade and used without further purification. The water used in the preparation of all solutions was obtained from a Millipore Waters Milli-Q water purification system.

Photocatalytic Reaction. Vis(visible light)-induced photocatalytic reactions were conducted in a cylindrical glass vessel with a recycling water jacket to avoid overheating. To ensure a thorough mixing, 200 mL of solution was dispensed into the reactor with mechanical stirring before and during the illumination. The suspension was irradiated by a 300 W Xe lamp (Beijing Perfectlight Co Ltd.), which emits both UV and visible light over a wide wavelength. To limit the irradiation wavelength, the light beam was passed through both UV cutoff and other filters of varied wavelength (420, 435, 450, 500 nm). For UV-induced photocatalytic reactions, they were conducted in a Rayonet RPR-200 photochemical reactor manufactured by the Southern New England Ultraviolet Co. Six phosphor-coated low-pressure mercury lamps at 350 nm were installed on the photoreactor. Samples were withdrawn at a predetermined interval and were filtered through a 0.2 μm PTFE membrane to keep the particles free from the solution prior to quantification. All experiments were carried out at room temperature (air-conditioned) at 23 °C in duplicate.

Characterization. Photocurrent generation was measured with a TiO_2/ITO (indium tin oxide) electrode immersed in an aqueous solution of H_2O_2. For preparing the TiO_2/ITO electrode, the ITO plates were first cleaned by sonication in acetone, ethanol, and distilled deionized water (DDW) for 30 min, respectively. Then ITO plates were spin-coated with TiO_2 film from a 25 g/L P25 ethanol suspension with the addition of 25 g/L glycerol. The TiO_2-coated ITO plates were calcined at 450 °C for 30 min to burn off organics and bind the TiO_2 film to the ITO plate. The TiO_2/ITO electrode, a saturated calomel electrode (SCE), and Pt plate were immersed in the reactor as working, reference, and counter electrodes, respectively. Photocurrents were recorded in aqueous solution with or without H_2O_2 as a function of elapsed time with application of a potential (+0.5 V vs SCE) using a potentiostat (VersaSTAT 3) connected to a computer. Photo intensity was measured by a photo detector (UP 19K-15S-H5-DO, Gentec-EO, Canada) connected to a computer.

Chemical Analysis. The LNR remaining after photoreaction was determined by HPLC (Waters). The system consisted of a Waters 515 HPLC pump, Waters 2487 Dual λ Absorbance Detector, an Agilent Hypersil ODS column (5 μm, 0.46 × 25 cm), and Waters 717plus Autosampler. The maximum adsorption wavelength (λ_{max}) was selected as 246 nm for LNR. A mixture of 60% acetonitrile and 40% water was used as the mobile phase running at a flow rate of 1 mL/min. Intermediate compounds for which standards are not available commercially were quantified in terms of ion intensity relative to the initial LNR concentration for comparison. This approximation is acceptable on the basis of the fact that the UV absorbance may be ascribed to the resonance structure of the ring, which is basically identical (*22*).

The identification of intermediates was carried out at an initial [LNR] of 0.3 mM. A Thermo Quest Finnigan LCQ Duo mass spectrometer system was used to identify the reaction intermediates; it consisted of a PDA-UV detector and an electrospray ionization with a quadrupole ion-trap mass spectrometer operating at a negative mode. The mobile phase was a mixture of (A) 5 mM ammonia acetate (pH 4.6) and (B) acetonitrile (100%). The composition of the mobile phase

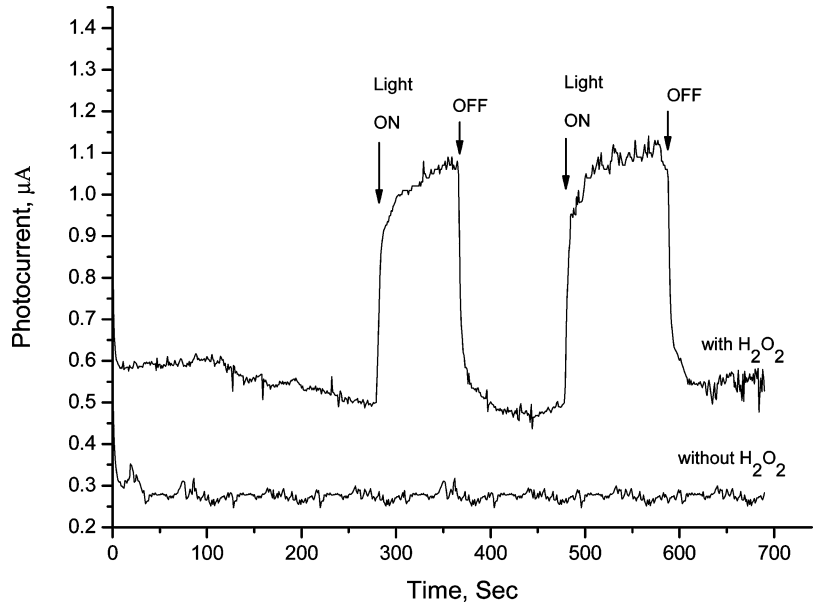

FIGURE 3. Visible-light-induced current (Iph) generation on a TiO_2/ITO electrode in water with or without H_2O_2 (the concentration of H_2O_2 solution is 0.03 M).

was changed according to the following gradient: 95% of A was kept during the first 2 min. From 2 to 26 min, B was steadily increased from 5% to 95%. From 26 to 27 min, B was kept at 95%. Finally, the mobile phase turned to the initial composition until the end of the run.

The generation of chloride, nitrite, and nitrate ions was monitored by the ion chromatograph (Dionex Series 4500i) composed of an anion column (Dionex IonPac AS14 (4 mm × 250 mm)), Dionex CD25 conductivity detector, and Dionex AS 40 automated sampler. A mixture of 1 mM $NaHCO_3$ and 3.5 mM Na_2CO_3 was used as the mobile phase eluting at 1 mL min^{-1}. For the quantification of the ammonium ion produced during the reaction, Dionex IonPac CS12 (4 mm × 250 mm) was used as a cation column and 0.022 M methane sulfonic acid (MSA) was used as the mobile phase eluting at 1 mL min^{-1}. The total organic carbon (TOC) was analyzed by a Shimadzu TOC-5000A analyzer equipped with an ASI-5000A autosampler to determine the mineralization of the organic pollutants during this process. The H_2O_2 concentration in the bulk solution was measured by means of UV−visible light absorbance spectroscopy at 408 nm (*23*).

Results and Discussion

LNR Degradation in Various Systems. Many studies have demonstrated that, under UV irradiation, H_2O_2 plays a dual role in enhancing the TiO_2-based photocatalytic degradation of organic compounds by acting either as an electron scavenger to prevent the recombination of e^- and h^+ or as a direct source of hydroxyl radicals (*24*−*27*). However, under visible light, the mechanism behind the degradation of organic compounds in the system of TiO_2/H_2O_2 is still not well-defined.

In this section, the degradation of LNR was investigated under various conditions including the presence or absence of TiO_2, the processes with or without H_2O_2, and the use of visible light irradiation or in the dark. As shown in Figure 1, it is interesting to note that no decay of LNR was observed in the systems of TiO_2/H_2O_2 (in the dark), TiO_2 with or without purging O_2 under the irradiation of visible light (420 nm), and Vis/H_2O_2 after 5 h of reaction. However, in the system of TiO_2/H_2O_2 under visible light (420 nm), more than 70% decay of LNR was observed.

No LNR decay was observed in TiO_2 suspension under the irradiation of visible light even with the purge of O_2 (a well-known electron acceptor) indicating no trace of UV light leaking into the reactor and no electron−hole pairs are generated in this system. It is expected that no LNR degradation was achieved in the system of H_2O_2/Vis because direct dissociation of H_2O_2 to $^{\bullet}OH$ can be attained only through absorbing UV light ($\lambda < 320$ nm). It has been reported that the degradation of methylene blue can be accomplished in the presence of H_2O_2-pretreated TiO_2 in the dark, which was ascribed to the formation of a stable oxidant—titanium peroxide—on the surface of TiO_2 particles (*11*). In the presence of H_2O_2, the −OOH groups of H_2O_2 substitute for the −OH groups of basic ≡TiOH, leading to the generation of a yellow surface complex—titanium peroxide (*9, 12*). It has also been reported that the interaction between H_2O_2 and rutile TiO_2 can form surface O_2^- anions and S = 1 triplet radical anion pairs (*28*). However, no LNR decay was observed in the TiO_2/H_2O_2 system in the dark in this study. This may suggest that the oxidizing power of both titanium peroxide and radical anions is too weak to effectively oxidize LNR.

Photocatalystic Degradation Mechanism of LNR under Visible Light. It was interesting to observe a synergistic effect in the system of TiO_2/H_2O_2/Vis for the decomposition of LNR. This synergistic effect may be rationalized by the following: (1) The interaction between H_2O_2 and TiO_2 leads to the formation of titanium peroxide complex and various radical anions on the TiO_2 surface which may act as oxidizing species

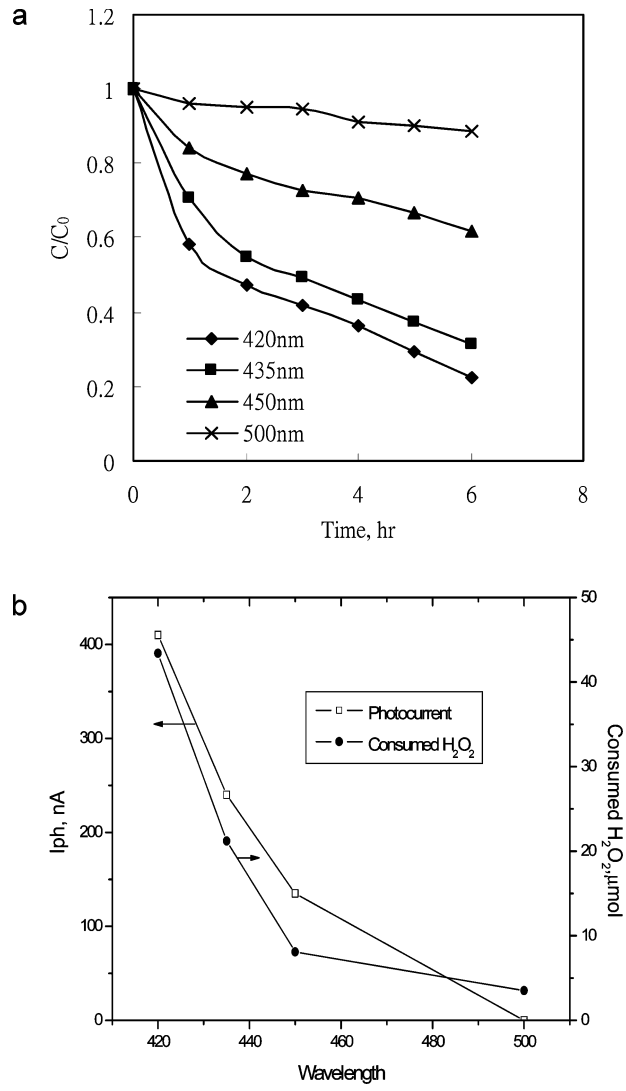

FIGURE 4. (a) Effect of wavelength of visible light on the LNR decay rate (initial LNR concentration is 0.1 mM, TiO_2 loading is 0.6 g/L, the initial concentration of H_2O_2 is 10 mM, initial pH value is 6.0). (b) *I*ph and the H_2O_2 consumption are compared as a function of the wavelength.

with the assistance of visible light (*9*). (2) Titanium peroxide complex on the TiO_2 surface extends the photoresponse of TiO_2 to the visible region, leading to the visible-light-induced surface electron transfer from surface complexes to the conduction band of TiO_2. The electrons on the conduction band of TiO_2 initiate the decomposition of H_2O_2, which gives rise to the generation of hydroxyl radicals (eq 1) (*10*).

$$H_2O_2 + e_{transfer}^- \rightarrow {}^{\bullet}OH + OH^- \qquad (1)$$

where $e_{transfer}^-$ is the electron transferred from surface complexes to the conduction band of TiO_2.

To investigate the photodegradation mechanism of LNR, three selective radical scavengers were utilized to assess the contribution of various radicals or other oxidizing species to the LNR decay. Bicarbonate and *tert*-butanol selectively quench hydroxyl radical while azide reacts with both singlet oxygen and hydroxyl radical (*29*). The addition of 100 mg/L bicarbonate and azide almost resulted in the 100% inhibition of the LNR degradation in this process; 100 mg/L tert-butanol caused a significant reduction in the LNR removal (decrease from 64% to 28% at fourth hour after using the quencher) while 3 g/L tert-butanol completely hinders the LNR deg-

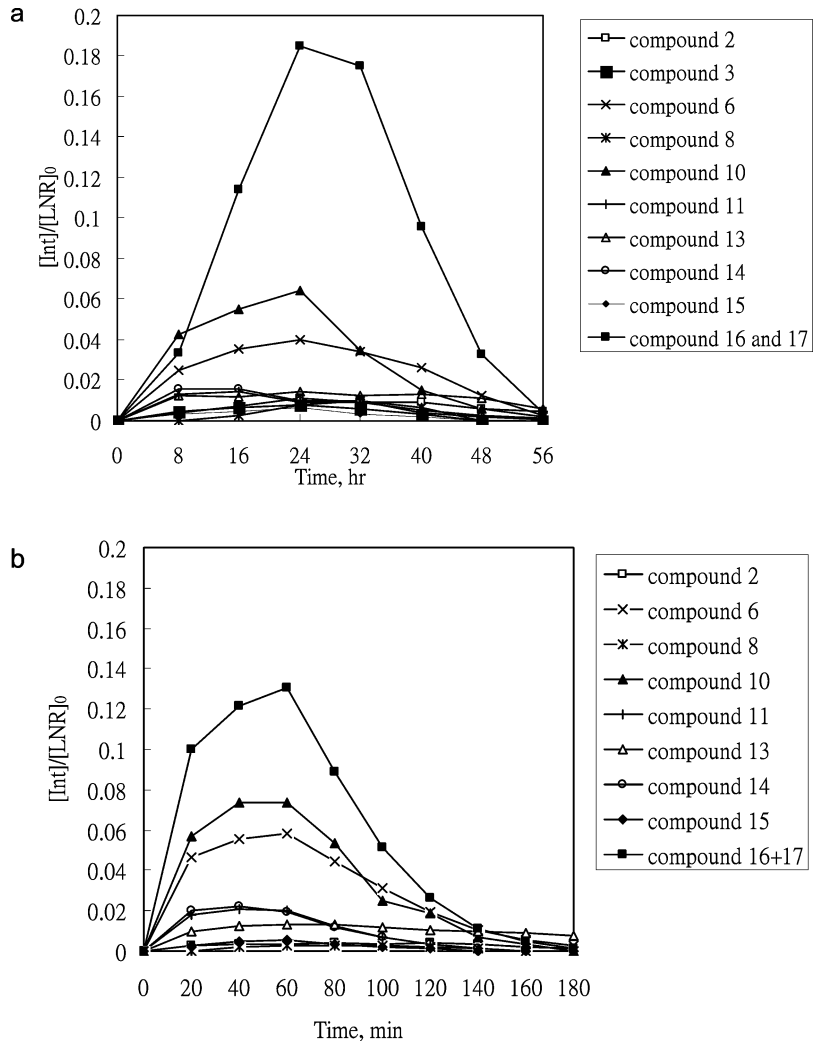

FIGURE 5. (a) Evolution profile of intermediates generated in Vis/TiO_2/H_2O_2 system. (b) Evolution profile of intermediates produced in UV/TiO_2 system. (initial concentration of LNR is 0.25 mM, initial concentration of H_2O_2 is 10 mM, initial pH value is 6.0; for UV/TiO2 system, six 350 nm UV lamps were used).

radation (see Figure 2), indicating that the LNR decay is likely dominated by the oxidation of hydroxyl radicals. It is interesting to note the addition of 100 mg/L bicarbonate retards the LNR degradation more effectively than 100 mg/L bicarbonate does although *tert*-butanol is more reactive toward OH radicals than bicarbonate. This may be because bicarbonate can not only compete for hydroxyl radicals with LNR but also competes for the adsorption sites on the TiO_2 surface with H_2O_2 and LNR. It has been reported that the anions exerted an inhibing effect on the photocatalytic degradation of organic pollutants due to the occurrence of the competitive adsorption (*30*).

It was proposed that the titanium peroxide complex formed on the surface of TiO_2 can be excited by visible light to produce electrons which can be transferred to the conduction band of TiO_2 and subsequently initiate the decomposition of H_2O_2 to produce hydroxyl radicals in the study of Li et al. (*10*). However, the production of electrons was not confirmed in their study. Thus, to investigate if electrons can be generated in this system, photocurrent generation was monitored from a TiO_2/ITO electrode immersed in aqueous 0.03 M H_2O_2 solution or DDW. The time profiles of photocurrents generated under visible light ($\lambda = 420 \pm 10$ nm) irradiation are demonstrated in Figure 3. When the visible light is on, the generation of around 410 nA photocurrent can be observed in aqueous H_2O_2 solution while no photocurrent is produced in DDW, indicating only the surface complex can be excited by visible light to generate an electron which is transferred to the electrode to generate visible-light-induced current (Iph).

Effect of Wavelength. The effect of wavelength of visible light on the LNR decay rate and the generation of photocurrent was also examined (Figure 4). Figure 4a shows that the degradation rate of LNR decreased with the increment of irradiation wavelength, where less than 12% LNR was removed by using 500 nm light after 6 h of irradiation. Figure 4b demonstrates the generated photocurrent and the consumption of H_2O_2 after 6 h of reaction in the presence of H_2O_2 under different wavelength irradiations. It can be seen that the correlation between the generated photocurrent and the consumed H_2O_2 is well established under various wavelengths; the shorter the wavelength (i.e., higher the energy), the higher the photocurrent, and subsequently the faster the consumption of H_2O_2. This suggests the electrons initiate the decomposition of H_2O_2. However, it is interesting to note that no photocurrent was generated under the irradiation of 500 nm visible light, although the formation of TiO_2 surface complexes could be extended to 550 nm visible light (*10*), and 3.6 μmol H_2O_2 was consumed after 6 h by 500 nm irradiation (from this study). This is likely because the signal of photocurrent produced is too weak to be detected by the potentiostat used in this study. In addition, the light intensity has also been measured in this study. The photo intensity at different wavelength is 178.6, 164.3, 167.8, and

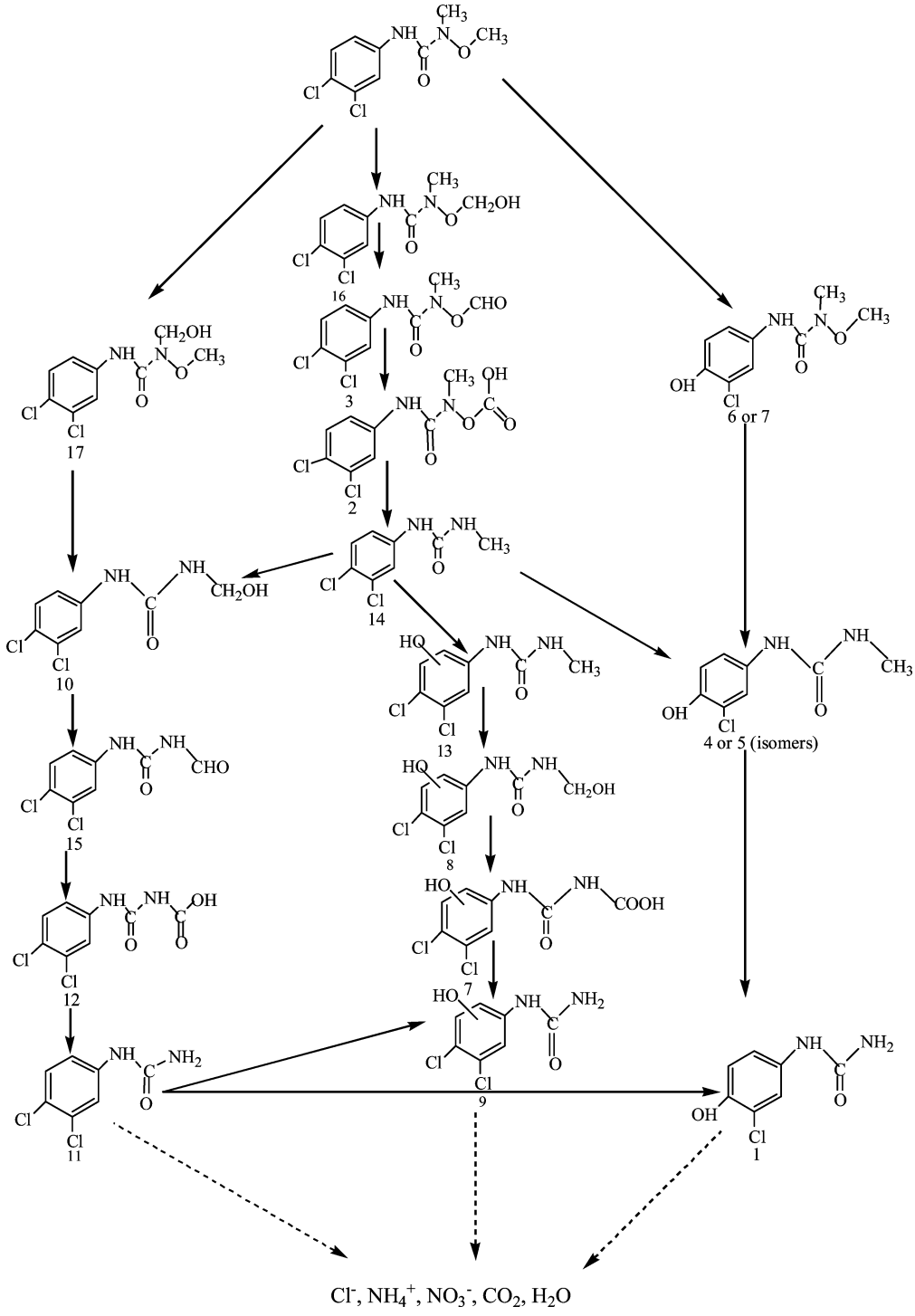

FIGURE 6. Degradation pathways of LNR for both Vis/TiO_2/H_2O_2 and UV/TiO_2 processes (dashed arrow represents reactants that could take more than one step to reach the products).

203.6 Wm^{2-} for 420, 435, 450, and 500 nm, respectively. Although the photo intensity is the highest at 500 nm, the weak absorbance of titanium peroxide complex at 500 nm (*10*) results in its weak response to light at this wavelength.

Photocatalytic Degradation Pathway of LNR under Visible Light or UV Irradiation. It is believed that hydroxyl radicals play a key role in the decomposition of organic compounds by UV/TiO_2 process. The investigation on the transformation products of LNR produced both in visible light and UV-induced photocatalytic process may cast a bright light on the degradation mechanism of LNR by TiO_2/H_2O_2/Vis process. The same concentration of LNR was degraded under irradiation of UV or visible light, where 16 and 17 intermediates were identified during the process on the basis of the molecular ions and mass fragment ions detected by MS spectrum for UV and visible light, respectively. The information on the intermediates including the mass of deprotonated ion ($[M - H]^+$) of the daughter compounds, the proposed molecular structure, the relative abundances, and the proposed fragments is summarized (see Table 1 in the Supporting Information). Actually, $[M + acetate]^-$ ions were obtained as a base peak of the mass spectra for most intermediates and LNR due to 5 mM ammonium acetate being used as mobile phase and negative-ion mode being employed in this study (*31*). The evolution profiles of major intermediates were organized and are shown in Figure 5a

and b (trace intermediates not included). As indicated in Figure 5, the formation/degradation profiles of the intermediates generated during these two processes are quite similar. It was also found that the decay of LNR was involved with *N*-demethoxylation and *N*-demethylation through alkylic-oxidation, dechlorination (hydroxylation at the chlorine site), and hydroxylation of the benzene ring in both processes. Direct dechlorination (no hydroxylation at the chlorine site) reported by other researchers (*21*) was not observed in this study. Until now, it has been believed that hydroxyl radicals also play a predominant role in Vis/TiO_2/H_2O_2 process similar to that in UV/TiO_2 process for the LNR decay. It can also be believed LNR suffers the same decay pathway by both Vis/TiO_2/H_2O_2 and UV/TiO_2 processes.

Therefore, the degradation pathway of LNR by Vis/TiO_2/H_2O_2 or UV/TiO_2 process was proposed on the basis of the profile analysis as illustrated in Figure 6. The decomposition of LNR was initiated by the attack of $OH^{\bullet}$ on the chlorine site of the benzene ring, *N*-terminus methyl, and methoxyl groups, leading to the generation of compounds 6, 16, and 17, respectively at the first step. The emergence of compound 6 was accompanied by the release of chlorine at the beginning of the reaction, which has been quantified (see Figure S2 in the Supporting Information). The oxidation of *N*-terminus methoxyl group of compound 16 led to the formation of compounds 2, 3, and 14 through dealkylation (alkylic side chain cleavage). The direct demethoxylation of compounds 6 and 17 resulted in the generation of compounds 4 or 5 and 10, respectively. Compound 10 is believed to have another source (the oxidation of *N*-terminus methyl of compound 14), which gives rise to high yield of compound 10 at the beginning of the reaction as demonstrated in Figure 5. In addition, dechlorination of compound 14 (hydroxylation at the chlorine site) also could form compounds 4 or 5, which was confirmed by an individual test using the standard of compound 14 as the initial probe in Vis/TiO_2/H_2O_2 system. This individual test also verified that 13.6% of compound 14 was transformed into compound 13 while 4.2% of compound 14 was converted to compound 4 and 5 after 7 h of reaction by Vis/TiO_2/H_2O_2 process (data not shown), which may rationalize higher yield of compound 13 than compounds 4 and 5 although compound 14 is the only possible source of compound 13. The further *N*-terminus oxidation of compound 10 produced compounds 15, 12, and 11 while the *N*-terminus oxidation of compound 13 caused the generation of compounds 8, 7, and 9. Compound 1 is believed to come from the *N*-terminus demethylation of compound 4. It should be noted that compound 13 may not be the only source responsible for the formation of compound 9, while compound 4 may not be the only source contributed to the production of compound 1. Compound 11 can also contribute to the yield of compound 1 and 9 through dechlorination (hydroxylation at the chlorine site on the benzene ring) and direct hydroxylation on the benzene ring without dechlorination, respectively, which was confirmed by an additional test using the compound 11 as the initial probe compound in this process. It was believed that 2,3-dichloroaniline was the terminal product of LNR decomposition (*19*). However, it was not detected in this study.

All intermediates were categorized into alkylic-oxidation derivatives (AOD), dechlorination-hydroxylation derivatives (DHD), and derivatives from the hydroxylation of benzene ring (HBD). To elucidate the major mechanism involved in these two processes, the transformation of LNR, the intermediates (in terms of AODs, DHDs, and HBDs), and the mass balance of benzene ring were reorganized and incorporated in Figure 7a and b. Figure 7 shows the concentration of AODs is much higher than that of DHDs and HBDs, indicating alkylic-oxidation is a dominant degradation mechanism while dechlorination (hydroxylation at the chlorine site) and

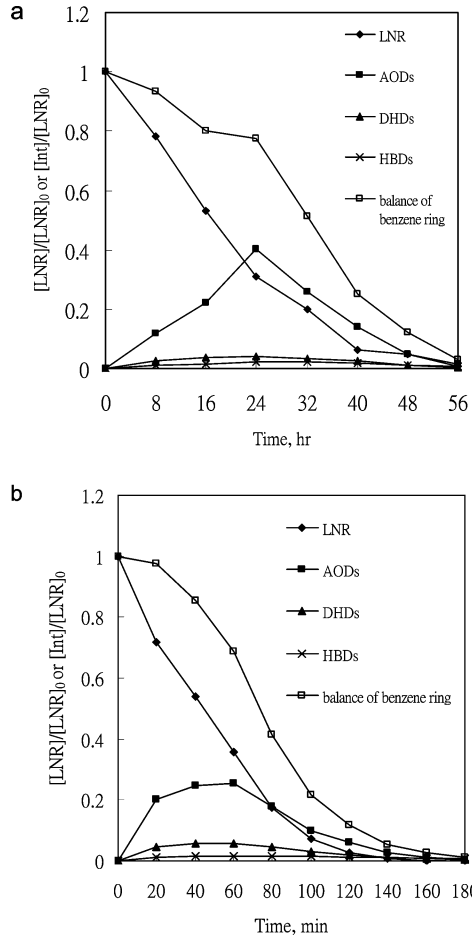

FIGURE 7. (a) Process summary of Vis/TiO_2/H_2O_2 (where [Int] stands for the concentration of intermediates). (b) Process summary of UV/TiO_2 (where [Int] stands for the concentration of intermediates).

hydroxylation of the aromatic ring are minor in terms of LNR decay in both UV/TiO_2 and Vis/TiO_2/H_2O_2 processes. This can be rationalized by the following: the disubstitution of the phenyl ring by chlorine atoms lowers its susceptibility toward any electrophilic or radical attack due to electron-drawing property of chlorine leading to lower electron density on the benzene ring, resulting in the attack on the urea *N*-terminus group being more competitive.

The evolution of chloride, ammonium, nitrate, and TOC was also monitored during the LNR decay reaction by Vis/TiO_2/H_2O_2 process (see Figure S1). Nearly 70% chlorine and 37% nitrogen were released after 56 h of reaction as shown in Figure S1. Judging from the mass balance of benzene ring in Figure 7, ring-opening was completed at the end of the reaction. However, only around 32% TOC was removed (see Figure S1). This suggests all aromatic compounds were broken down into simple aliphatic acids, which account for the dominating part of TOC. Furthermore, it is interesting to note that the TiO_2 particles sunk down to the bottom of the reactor automatically in 10 min right after the stirring was stopped. The release of chlorine due to dechlorination−hydroxylation and the generation of organic acid led to pH level dropping from 6.0 to 3.07 in Vis/TiO_2/H_2O_2 system after 56 h (data are not shown). At pH 3.07, the TiO_2 surface is positively charged ($Ti-OH_2^+$), which may favor the adsorption of the anions released during the reaction. The anion adsorption may weaken the repulsion of TiO_2 particles positively charged and start the aggregation of TiO_2 particles.

In summary, hydroxyl radicals are believed to play a dominant role in LNR degradation in Vis/TiO_2/H_2O_2

system, judging from LNR decay being completely hampered after the application of radical scavengers as well as the comparison of the identical intermediates and decay mechanism between Vis/TiO_2/H_2O_2 and UV/TiO_2 processes. The generation of electrons was first confirmed by monitoring photocurrent while TiO_2-coated ITO electrode was immersed in H_2O_2 solution. Subsequent reaction between electron and H_2O_2 can produce hydroxyl radicals. It is believable that Vis/TiO_2/H_2O_2 process is cost efficient and practically applicable in the removal of persistent organic contaminants in natural waters since it can work under the irradiation of visible light which accounts for a much larger part of solar light than UV.

Acknowledgments

We are grateful to the University Research Fund (RGTN) from the Hong Kong Polytechnic University for financial support.

Supporting Information Available

Table 1 shows the molecular structure, retention time, and main fragments of the identified degradation products determined by LC/ESI-MS; Figure 1 demonstrates the evolution of TOC, chloride, ammonium, and nitrate ions during Vis-induced photocatalytic reaction. This information is available free of charge via the Internet at http://pubs.acs.org/.

Literature Cited

(1) Augugliaro, V.; Loddo, V.; Palmisano, L.; Schiavello, M. Performance of heterogeneous photocatalytic systems - Influence of operational variables on photoactivity of aqueous suspension of TiO_2. *J. Catal.* **1995**, *153* (1), 32–40.

(2) Hoffmann, M. R.; Martin, S. T.; Choi, W. Y.; Bahnemann, D. W. Environmental applications of semiconductor photocatalysis. *Chem. Rev.* **1995**, *95* (1), 69–96.

(3) Ding, Z.; Lu, G. Q.; Greenfield, P. F. Role of the crystallite phase of TiO_2 in heterogeneous photocatalysis for phenol oxidation in water. *J. Phys. Chem. B* **2000**, *104* (19), 4815–4820.

(4) Lin, J.; Yu, J. C.; Lo, D.; Lam, S. K. Photocatalytic activity of rutile $Ti_{1-x}Sn_xO_2$ solid solutions. *J. Catal.* **1999**, *183* (2), 368–372.

(5) Asahi, R.; Morikawa, T.; Ohwaki, T.; Aoki, K.; Taga, Y. Visible-light photocatalysis in nitrogen-doped titanium oxides. *Science* **2001**, *293* (5528), 269–271.

(6) Cho, Y. M.; Choi, W. Y.; Lee, C. H.; Hyeon, T.; Lee, H. I. Visible light-induced degradation of carbon tetrachloride on dye-sensitized TiO_2. *Environ. Sci. Technol.* **2001**, *35* (5), 966–970.

(7) Huang, Y.; Zheng, Z.; Ai, Z. H.; Zhang, L. Z.; Fan, X. X.; Zou, Z. G. Core-shell microspherical $Ti_{1-x}Zr_xO_2$ solid solution photocatalysts directly from ultrasonic spray pyrolysis. *J. Phys. Chem. B* **2006**, *110* (39), 19323–19328.

(8) Zaleska, A.; Sobczak, J. W.; Grabowska, E.; Hupka, J. Preparation and photocatalytic activity of boron-modified TiO_2 under UV and visible light. *Appl. Catal. B, Environ.* **2008**, *78* (1−2), 92–100.

(9) Ohno, T.; Masaki, Y.; Hirayama, S.; Matsumura, M. TiO_2-photocatalyzed epoxidation of 1-decene by H_2O_2 under visible light. *J. Catal.* **2001**, *204* (1), 163–168.

(10) Li, X. Z.; Chen, C. C.; Zhao, J. C. Mechanism of photodecomposition of H_2O_2 on TiO_2 surfaces under visible light irradiation. *Langmuir* **2001**, *17* (13), 4118–4122.

(11) Ogino, C.; Dadjour, M. F.; Iida, Y.; Shimizu, N. Decolorization of methylene blue in aqueous suspensions of titanium peroxide. *J. Hazard. Mater.* **2008**, *153* (1−2), 551–556.

(12) Boonstra, A. H.; Mutsaers, C. Adsorption of hydrogen-peroxide on surface of titanium dioxide. *J. Phys. Chem.* **1975**, *79* (18), 1940–1943.

(13) Katsumata, H.; Kaneco, S.; Suzuki, T.; Ohta, K.; Yobiko, Y. Degradation of linuron in aqueous solution by the photo-Fenton reaction. *Chem. Eng. J.* **2005**, *108* (3), 269–276.

(14) Sorensen, S. R.; Rasmussen, J.; Jacobsen, C. S.; Jacobsen, O. S.; Juhler, R. K.; Aamand, J. Elucidating the key member of a linuron-mineralizing bacterial community by PCR and reverse transcription-PCR denaturing gradient gel electrophoresis 16S rRNA gene fingerprinting and cultivation. *Appl. Environ. Microbiol.* **2005**, *71* (7), 4144–4148.

(15) Benitez, F. J.; Acero, J. L.; Real, F. J.; Garcia, C. Removal of phenylurea herbicides in ultrapure water by ultrafiltration and nanofiltration processes. *Water Res.* **2009**, *43* (2), 267–276.

(16) Dejonghe, W.; Berteloot, E.; Goris, J.; Boon, N.; Crul, K.; Maertens, S.; Hofte, M.; De Vos, P.; Verstraete, W.; Top, E. M. Synergistic degradation of linuron by a bacterial consortium and isolation of a single linuron-degrading Variovorax strain. *Appl. Environ. Microbiol.* **2003**, *69* (3), 1532–1541.

(17) Faure, V.; Boule, P. Phototransformation of linuron and chlorbromuron in aqueous solution. *Pestic. Sci.* **1997**, *51* (4), 413–418.

(18) Tahmasseb, L. A.; Nelieu, S.; Kerhoas, L.; Einhorn, J. Ozonation of chlorophenylurea pesticides in water: reaction monitoring and degradation pathways. *Sci. Total Environ.* **2002**, *291* (1−3), 33–44.

(19) Farre, M. J.; Brosillon, S.; Domenech, X.; Peral, J. Evaluation of the intermediates generated during the degradation of Diuron and Linuron herbicides by the photo-Fenton reaction. *J. Photochem. Photobiol. A* **2007**, *189* (2−3), 364–373.

(20) Benitez, F. J.; Real, F. J.; Acero, J. L.; Garcia, C. Photochemical oxidation processes for the elimination of phenyl-urea herbicides in waters. *J. Hazard. Mater.* **2006**, *138* (2), 278–287.

(21) Lopez, M. C.; Fernandez, M. I.; Rodriguez, S.; Santaballa, J. A.; Steenken, S.; Vulliet, E. Mechanisms of direct and TiO_2-photocatalysed UV degradation of phenylurea herbicides. *Chemphyschem* **2005**, *6* (10), 2064–2074.

(22) Adams, C. D.; Randtke, S. J. Ozonation by-products of atrazine in synthetic and natural-waters. *Environ. Sci. Technol.* **1992**, *26* (11), 2218–2227.

(23) Eisenberg, G. M. Colorimetric determination of hydrogen peroxide. *Ind. Eng. Chem.-Anal. Ed.* **1943**, *15*, 327–328.

(24) Poulios, I.; Micropoulou, E.; Panou, R.; Kostopoulou, E. Photooxidation of eosin Y in the presence of semiconducting oxides. *Appl. Catal. B, Environ.* **2003**, *41* (4), 345–355.

(25) Kaniou, S.; Pitarakis, K.; Barlagianni, I.; Poulios, I. Photocatalytic oxidation of sulfamethazine. *Chemosphere* **2005**, *60* (3), 372–380.

(26) Wong, C. C.; Chu, W. The hydrogen peroxide-assisted photocatalytic degradation of alachlor in TiO_2 suspensions. *Environ. Sci. Technol.* **2003**, *37* (10), 2310–2316.

(27) Nienow, A. M.; Bezares-Cruz, J. C.; Poyer, I. C.; Hua, I.; Jafvert, C. T. Hydrogen peroxide-assisted UV photodegradation of Lindane. *Chemosphere* **2008**, *72* (11), 1700–1705.

(28) Murphy, D. M.; Griffiths, E. W.; Rowlands, C. C.; Hancock, F. E.; Giamello, E. EPR study of the H_2O_2 interaction with TiO_2; evidence for a novel S=1 surface radical pair. *Chem. Commun.* **1997**, (22), 2177–2178.

(29) Xu, Z. H.; Jing, C. Y.; Li, F. S.; Meng, X. G. Mechanisms of photocatalytical degradation of monomethylarsonic and dimethylarsinic acids using nanocrystalline titanium dioxide. *Environ. Sci. Technol.* **2008**, *42* (7), 2349–2354.

(30) Liang, H. C.; Li, X. Z.; Yang, Y. H.; Sze, K. H. Effects of dissolved oxygen, pH, and anions on the 2,3-dichlorophenol degradation by photocatalytic reaction with anodic TiO_2 nanotube films. *Chemosphere* **2008**, *73* (5), 805–812.

(31) Barcelo, D.; Albaiges, J. Characterization of organo-phosphorus compounds and phenylurea herbicides by positive and negative-ion thermospray liquid-chromatography mass-spectrometry. *J. Chromatogr.* **1989**, *474* (1), 163–173.

ES901333H